



NRC Publications Archive Archives des publications du CNRC

Optically timed submillimeter time-of-flight mass spectrometry

Dooley, Patrick W.; Bhardwaj, V. Ravi; Rayner, David M.; Corkum, Paul B.

This publication could be one of several versions: author's original, accepted manuscript or the publisher's version. / La version de cette publication peut être l'une des suivantes : la version prépublication de l'auteur, la version acceptée du manuscrit ou la version de l'éditeur.

For the publisher's version, please access the DOI link below. / Pour consulter la version de l'éditeur, utilisez le lien DOI ci-dessous.

Publisher's version / Version de l'éditeur:

<https://doi.org/10.1021/ac034621x>

Analytical Chemistry, 76, 2, pp. 262-266, 2004

NRC Publications Record / Notice d'Archives des publications de CNRC:

<https://nrc-publications.canada.ca/eng/view/object/?id=f935144e-f6e5-4f6e-9a0f-7289cfb0b3d2>

<https://publications-cnrc.canada.ca/fra/voir/objet/?id=f935144e-f6e5-4f6e-9a0f-7289cfb0b3d2>

Access and use of this website and the material on it are subject to the Terms and Conditions set forth at

<https://nrc-publications.canada.ca/eng/copyright>

READ THESE TERMS AND CONDITIONS CAREFULLY BEFORE USING THIS WEBSITE.

L'accès à ce site Web et l'utilisation de son contenu sont assujettis aux conditions présentées dans le site

<https://publications-cnrc.canada.ca/fra/droits>

LISEZ CES CONDITIONS ATTENTIVEMENT AVANT D'UTILISER CE SITE WEB.

Questions? Contact the NRC Publications Archive team at

PublicationsArchive-ArchivesPublications@nrc-cnrc.gc.ca. If you wish to email the authors directly, please see the first page of the publication for their contact information.

Vous avez des questions? Nous pouvons vous aider. Pour communiquer directement avec un auteur, consultez la première page de la revue dans laquelle son article a été publié afin de trouver ses coordonnées. Si vous n'arrivez pas à les repérer, communiquez avec nous à PublicationsArchive-ArchivesPublications@nrc-cnrc.gc.ca.



Articles

Optically Timed Submillimeter Time-of-Flight Mass Spectrometry

Patrick W. Dooley,^{†,‡} V. Ravi Bhardwaj,[†] David M. Rayner,[†] and Paul B. Corkum^{*,†,‡}

Steacie Institute for Molecular Sciences, National Research Council of Canada, Ottawa, Ontario, K1A 0R6, Canada, and Department of Physics & Astronomy, McMaster University, Hamilton, Ontario, L8S 4M1, Canada

We demonstrate that using intense femtosecond laser pulses to optically time ion flight can lead to a miniature time-of-flight mass spectrometer. After laser ionization, the molecular ion is accelerated by a static electric field and detected using a second, delayed laser pulse. The relative positions of the two laser foci determine the ion flight distance while the time separation of the laser pulses fixes the ion flight time. We mass-resolve CS₂ or C₆H₆ isotopes after a flight distance of 360 μm using either double ionization or Coulomb explosion detection.

Femtosecond pulses have been of interest in mass spectrometry primarily for their proposed ability to ionize molecules with little or no fragmentation.¹ However, recent research calls this prospect into question.² For organic molecules of intermediate size, at least, it appears that femtosecond pulses and electron impact methods often produce similar fragmentation behavior.² Nevertheless, femtosecond pulses offer additional benefits of considerable importance for mass analysis, as detailed below.

Like electron beam ionization, strong-field ionization using femtosecond laser pulses is nonresonant and universal. Unlike electron beam methods, strong-field ionization can be highly efficient (~100%) and localized to a focal spot diameter of ~1 μm due to the nonlinearity of the light/matter interaction. Therefore, such pulses are well suited for miniature time-of-flight mass spectrometers whose mass resolution is determined by the ratio of the ion flight distance to the length of the ionization region along the flight direction. Miniature mass analyzers are of particular interest for applications such as spacecraft life support, pollution monitoring, and explosives detection.³

Intense femtosecond pulses can further ionize molecular ions. Depending on the pulse intensity, this can be controlled to remove one or more additional electrons and can lead to Coulomb explosion.^{4–8} Such localized postionization provides an optical method for detecting ions with high spatial resolution.

The time separation between two ultrashort pulses can be controlled with femtosecond precision. Hence, a dramatic improvement in the measurement of ion flight times can be achieved using optical rather than electronic timing. This eliminates the principal barrier to the realization of miniature time-of-flight mass spectrometers.

When used as a detection scheme, Coulomb explosion produces numerous ionic fragments that impinge upon a detector. This results in significant amplification of ion signal over parent ion detection. In contrast to conventional time-of-flight detection methods, this amplification increases with the size of the molecule.

We employ these properties of femtosecond pulses to time ion flight optically. In so doing, we show that the flight length of state-of-the-art miniature mass spectrometers can be reduced by 2 orders of magnitude.⁹ In addition, we demonstrate the feasibility of using Coulomb explosion to enhance the detection efficiency of such miniature devices.

Our optical approach involves focusing two temporally separated femtosecond pulses to positions less than 500 μm apart in the presence of a uniform, static electric field (Figure 1a). The pump pulse is focused to produce a highly localized packet of singly charged ions. The ions are accelerated toward the probe laser focus by a uniform electric field. En route to the probe focus, the ions separate spatially according to their masses. Consequently, different masses pass through the probe focus at different times. When the intense probe pulse arrives, it further ionizes any mass-selected cations present in its focal volume. Subsequent detection of highly charged molecular ions or fission fragments indicates that a specific mass existed in the sample, given by $m = eE\tau^2/2y$, where e is the unit of elementary charge, E is the external electric field strength, y is the focal spot separation along the electric field direction, and τ is the pump–probe delay.

(4) Hatherly, P. A.; Frasiniski, L. J.; Codling, K. *Chem. Phys. Lett.* **1988**, *149*, 477–481.

(5) Strickland, D. T.; Beaudoin, Y.; Dietrich, P.; Corkum, P. B.; *Phys. Rev. Lett.* **1992**, *68*, 2755–2758.

(6) Purnell, J.; Snyder, E. M.; Wei, S.; Castleman, A. W., Jr. *Chem. Phys. Lett.* **1994**, *229*, 333–339.

(7) Ivanov, M. Yu.; Seideman, T.; Corkum, P. B. *Phys. Rev. A* **1996**, *54*, 1541–1550.

(8) Hankin, S.; Villeneuve, D. M.; Corkum, P. B.; Rayner, D. M. *Phys. Rev. A* **2001**, *64*, 013405-1-12.

(9) Cotter, R. J.; Fancher, C.; Cornish, T. J. *J. Mass Spectrom.* **1999**, *34*, 1368–1372.

* Corresponding author: (e-mail) paul.corkum@nrc.ca; (fax) (613) 991-3437.

[†] National Research Council of Canada.

[‡] McMaster University.

(1) Ledingham, K. W. D.; Singhal, R. P. *Int. J. Mass Spectrom. Ion. Processes* **1997**, *163*, 149–168.

(2) Hankin, S.; Villeneuve, D.; Corkum, P. W.; Rayner, D. M. *Phys. Rev. Lett.* **2000**, *84*, 5082–5085.

(3) Badman, E. R.; Cooks, R. G. *J. Mass Spectrom.* **2000**, *35*, 659–671.

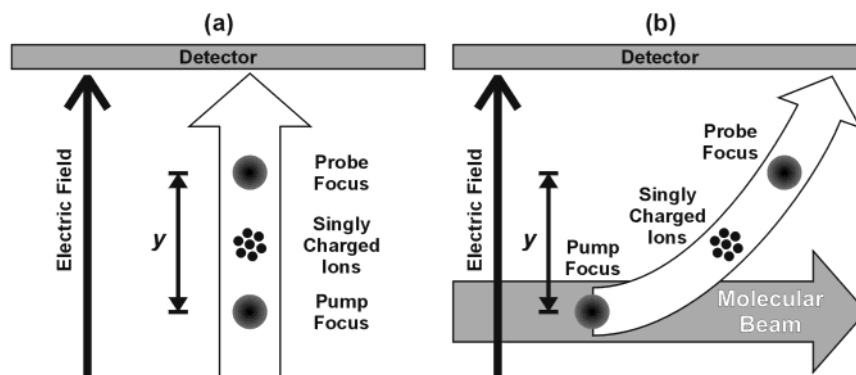


Figure 1. Optical timing of ion flight. (a) A packet of singly charged ions is produced in the pump laser focus. A uniform electric field accelerates the cations toward the probe laser focus, a distance y away. Upon its arrival, the probe pulse further ionizes any cations (of mass $m = eEr^2/2y$) present within its focal volume. Subsequent detection of multiply charged molecular ions or fission fragments indicates that molecules of mass $m = eEr^2/2y$ are present in the sample. (b) A pump pulse singly ionizes molecules moving with constant velocity within a molecular beam. The cations are accelerated out of the beam by a uniform electric field and follow parabolic trajectories. The probe pulse is focused at a location along a particular trajectory. As in (a), the delayed pulse probes for cations of mass $m = eEr^2/2y$ within its focal volume.

Note that the detector requirements in our scheme differ from those for standard time-of-flight configurations. Since we use the delay between the two laser pulses to optically time ion flight, the detector must only integrate charge. Moreover, ion mass information can be obtained by detecting either ions or electrons.

We can scan the mass probed by varying either the accelerating electric field or the pump–probe delay and spatial separation of the laser foci. In this work, we report results obtained by varying only the electric field.

To keep background ion signals to a minimum, neutral molecules must be kept out of the intense probe pulse's focal volume. This is most readily achieved by entraining the sample in a molecular beam and focusing the probe pulse outside of it. Orienting the molecular beam perpendicular to the electric field minimizes the distribution of initial ion velocities in the acceleration direction and improves mass resolution. In such a configuration, ion trajectories are parabolic but the dependence of the mass equation on y is unchanged (Figure 1b).

EXPERIMENTAL SECTION

We performed our proof-of-principle experiments using an existing electronically timed, constant-acceleration time-of-flight mass spectrometer equipped with a differentially pumped molecular beam source.¹⁰ This configuration enabled a detailed analysis of the ions and fragments produced by the probe laser but is not necessary for practical applications of the technique.

Molecular Beam. The background pressure in the interaction region was 10^{-9} mbar. The molecular beam was produced by a $100\text{-}\mu\text{m}$ pinhole backed by 40 mbar of gas and collimated by a piezoelectric slit. In the interaction region, the molecular beam was ribbonlike with a thickness of $40\ \mu\text{m}$ along the laser propagation direction and a width of 1.5 mm along the electric field direction. Molecules within the highly collimated beam had a measured mean velocity of 550 m/s and a transverse translational temperature of $\sim 1\ \mu\text{K}$.

Optical Configuration. The optical configuration is depicted in Figure 2. A regeneratively amplified Ti:sapphire laser system

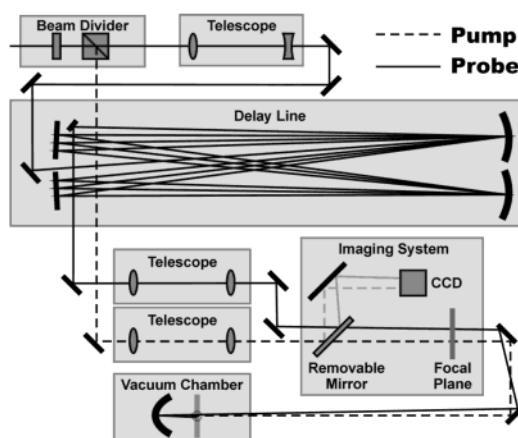


Figure 2. Optical configuration. The output from the amplified Ti:sapphire laser system was divided into pump and probe pulses. The probe pulse was focused at the input of the optical delay line by a telescope and refocused after each round trip by spherical mirrors. Both pulses were focused in a common vertical plane before entering the vacuum chamber. The relative separation of the external foci was determined by inserting a removable mirror to reflect them onto a CCD camera. Without the removable mirror in place, the intrachamber parabolic mirror imaged the external foci into/onto the edge of the molecular beam with a demagnification of $\sim 41:1$.

(not shown) operating at 800 nm produces $500\text{-}\mu\text{J}$, 50-fs-duration pulses at a repetition rate of 500 Hz. A half-wave plate/cube polarizer combination was used to divide the laser output into pump and probe pulses. To obtain pump–probe delays of $\sim 10^{-7}$ s, a delay line consisting of a pair of 2-m focal length spherical mirrors placed 4 m from two flat dielectric mirrors was constructed. The probe beam was focused at the input of the delay line and followed a bowtie path (56-m total length) as the concave mirrors repeatedly imaged the input focal spot onto the flat mirrors. The overall pump–probe delay was 203 ns.

The pump and probe pulses were focused to $\sim 8\text{-}\mu\text{m}$ -diameter spots by a parabolic mirror (50-mm focal length) mounted within the vacuum chamber. The probe focus was positioned $110\ \mu\text{m}$ (i.e., $550\ \text{m/s} \times 203\ \text{ns}$) downstream along the molecular beam direction from the pump focus and $y = 360\ \mu\text{m}$ closer to the detector (Figure 3). An imaging system (magnification $\sim 41:1$;

(10) Dooley, P. W.; Litvinyuk, I. V.; Lee, K. F.; Rayner, D. M.; Spanner, M.; Villeneuve, D. M.; Corkum, P. B. *Phys. Rev. A* **2003**, *68*, 023406.

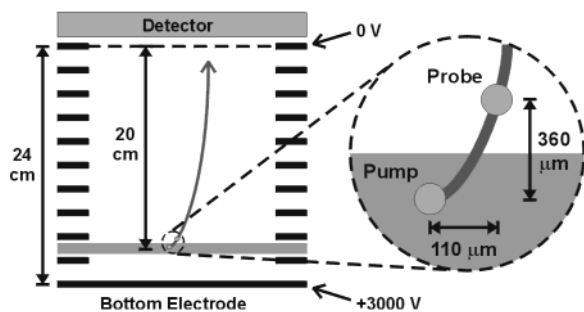


Figure 3. Positions of the laser foci. The pump pulse was focused into the molecular beam (gray horizontal stripe in figure). The probe focus was positioned (110 μm downstream from the pump focus and 360 μm nearer to the detector) on the edge of the molecular beam to coincide with a particular parabolic ion trajectory. Ions were accelerated using a large, existing time-of-flight mass spectrometer consisting of a 24-cm-long stack of electrode rings (black boxes in figure). A uniform ~ 125 V/cm ion acceleration field was produced by applying a ~ 3000 -V potential difference to the electrode stack. The potential difference between the closely spaced foci was only ~ 5 V.

Figure 2) was used to monitor the relative positions of the two foci during their adjustment.

Positioning of the foci relative to the molecular beam was achieved by translating the parabolic mirror. The pump focus was placed within the molecular beam while the probe focus was positioned on its edge. Given the universality of femtosecond laser ionization, probing is best performed in a region devoid of background gas. We achieved a gas density ratio of $\sim 20:1$ between the pump and probe foci.

External TOF-MS Configuration. Ions generated in the pump focal volume were accelerated by a uniform electric field (~ 125 V/cm) produced throughout our existing constant-acceleration time-of-flight mass spectrometer (mass resolution $m/\Delta m \approx 3000$; Figure 3). The spectrometer consists of a stack of ring electrodes (24 cm long) mounted within the vacuum chamber with apertures to accommodate the focusing mirror as well as the laser and molecular beams. This arrangement effectively represents a nested configuration in which the miniature optical spectrometer resides within the standard one.

Ion Detection. Ions were detected at the end of the electrode stack using a microchannel plate pair in combination with a conical anode. The ion signal was amplified, discriminated, and time-binned using a multichannel scaler with 500-ps temporal resolution. Note that the miniature spectrometer's mass resolution depends on the ion flight time between foci rather than the ion arrival time at the detector (Figure 1). Since the detector need only distinguish between singly charged parent ions and multiply charged ones (or fragments thereof), the probe focus–detector separation is largely irrelevant. In our proof-of-principle experiments, the 20-cm probe focus–detector separation imposed by our lengthy existing spectrometer was used for convenience (Figure 3). In an engineered miniature device, however, this separation could be easily submillimeter.

RESULTS

We now demonstrate our ability to perform mass analysis after an ion flight distance of only 360 μm using two different approaches. In each instance, a 30- μJ ($\sim 1 \times 10^{14}$ W/cm 2) pump pulse produced singly charged molecular ions. In the first

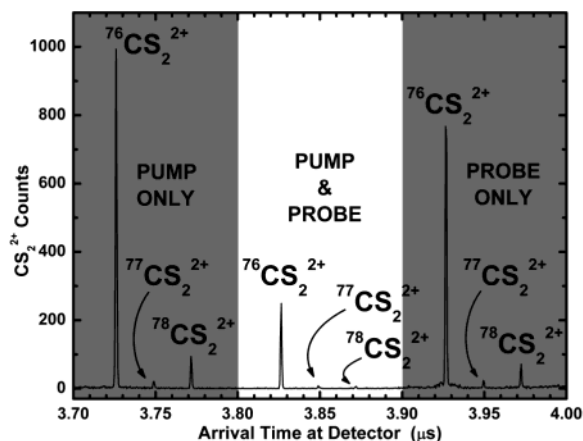


Figure 4. Spectrum of arrival times of CS_2^{2+} ions at the detector consisting of three triplets of peaks. Each peak within a triplet corresponds to a different isotope. The outer triplets (shaded regions) result from double ionization by either the pump pulse (leftmost triplet) or probe pulse (rightmost triplet), reflect natural isotopic abundances, and are separated by the pump–probe delay. The central triplet stems from consecutive one-electron removals in each of the pump and probe foci. Relative peak heights within the central triplet depend on focal spot separation and acceleration field.

approach, a 50- μJ ($\sim 1.7 \times 10^{14}$ W/cm 2) probe pulse was used to ionize the molecular cations and the production of doubly charged molecular ions was monitored. In the second approach, a more energetic 60- μJ ($\sim 2 \times 10^{14}$ W/cm 2) probe pulse was used to Coulomb explode the molecular cations. In each case, the positions of the foci and the pump–probe delay were held constant and the molecular mass was scanned by varying the acceleration voltage. We used CS_2 and C_6H_6 for these demonstrations.

Doubly Ionized Molecular Ion Detection. The universality of femtosecond ionization is both an asset and a liability. The pump pulse energy (30 μJ) was chosen to efficiently generate cations without excessive dication production. There are three possible sources of dications, and these are readily identified using our conventional mass spectrometer: (1) direct double ionization by the pump pulse, (2) direct double ionization by the probe pulse of molecules near the edge of the molecular beam, and (3) consecutive ionization by the pump and probe pulses. These three processes are manifested in the spectrum of CS_2^{2+} ion arrival times at the detector (Figure 4). Three triplets of peaks are in evidence, one for each production mechanism. The triplet corresponding to CS_2^{2+} produced by the pump pulse alone arrives first and illustrates the ~ 3.7 - μs ion flight time between the pump focus and the detector. Similarly, the triplet corresponding to CS_2^{2+} produced by the probe pulse alone arrives last. Its ~ 3.9 - μs detector arrival time is the sum of the 203-ns pump–probe delay and the ~ 3.7 - μs ion flight time between probe focus and the detector. Of interest is the central triplet, which results from consecutive ionization steps in each of the foci. Although the CS_2^{2+} ions of the central triplet are produced in the probe focus following the 203-ns pump–probe delay, they have a significant initial velocity oriented toward the detector. This stems from the precursor CS_2^+ ions' acceleration between the pump and probe foci. As a result, the consecutively ionized CS_2^{2+} ions arrive at the detector midway between their “pump only” and “probe only” counterparts.

The peaks of each triplet correspond to the isotopes of CS_2 ($^{76}\text{CS}_2$, $^{77}\text{CS}_2$, $^{78}\text{CS}_2$). The relative peak heights within the “pump

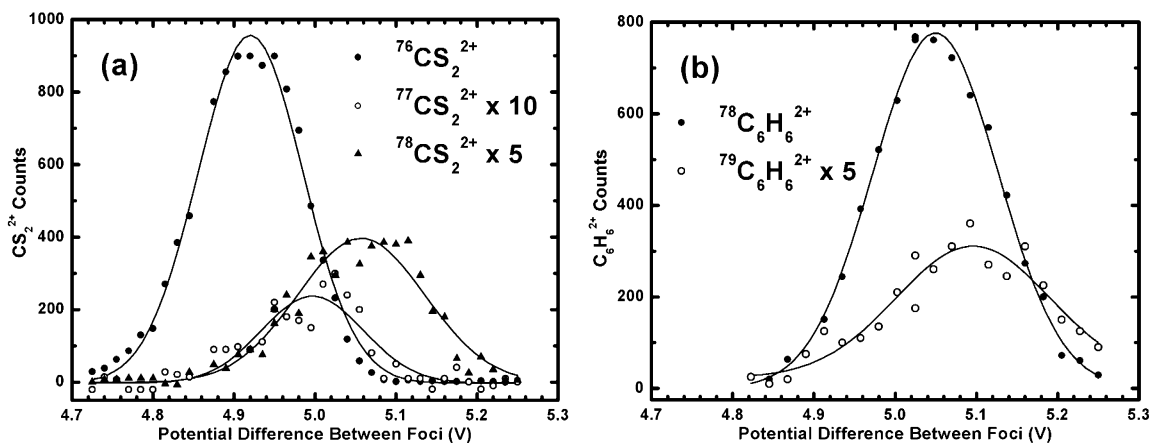


Figure 5. (a) Integrated $^{76}CS_2^{2+}$ (filled circles), $^{77}CS_2^{2+}$ (hollow circles), and $^{78}CS_2^{2+}$ (triangles) signals for the central triplet of Figure 4 as a function of potential difference between foci. For clarity, the magnitudes of the $^{77}CS_2^{2+}$ and $^{78}CS_2^{2+}$ signals have been increased by factors of 10 and 5, respectively. Gaussians fit to each data set have centers consistent with the mass equation $m = eE\tau^2/2y$ and heights reflecting relative isotopic abundances. (b) Results for $^{78}C_6H_6^{2+}$ (filled circles) and $^{79}C_6H_6^{2+}$ (hollow circles; plotted with a 5× magnitude enhancement) are consistent with both the mass equation and expected isotopic abundances.

only” and “probe only” triplets reflect the natural isotopic abundances of CS_2 . The central triplet is produced jointly by the pump and probe pulses and is therefore the signal of interest. However, the relative peak heights within this “pump–probe” triplet are different. This is because the accelerating voltage was chosen to place $^{76}CS_2^{2+}$ at the center of the second focus upon the arrival of the probe pulse. Hence, the $^{77}CS_2^{2+}$ and $^{78}CS_2^{2+}$ peaks are suppressed.

By varying the acceleration voltage, we sampled different isotopes within the probe focus. The pump–probe signal from the isotopes of CS_2^{2+} is shown in Figure 5a as a function of acceleration voltage. The relative heights of the isotope peaks approximate the natural abundances of CS_2 . The voltage at which each isotope signal maximizes is unique and is consistent with the predictions of the mass equation $m = eE\tau^2/2y$. This was also the case for the isotopes of $C_6H_6^{2+}$ (Figure 5b). We have therefore demonstrated the principle of optically timed mass spectrometry after an ion flight distance of just 360 μm with a mass resolution $m/\Delta m \approx 40$.

The achievable mass resolution is determined by the diameters of the foci relative to the ion flight distance. Since our pump and probe beams impinged upon the parabolic mirror at an angle, comatic aberration produced focal spot diameters ~ 2 times larger than the diffraction limit for our focusing conditions. Using diffraction-limited $f/1$ foci would yield a mass resolution $m/\Delta m \approx 320$. Alternatively, the ion flight distance could be reduced to $y \approx 45 \mu m$ without loss of mass resolution. In either case, the required pulse energies would be reduced by a factor of ~ 64 . An additional improvement in mass resolution should result if the acceleration field structure was modified to achieve space focusing.

Coulomb Explosion Detection. We now demonstrate a second approach to mass analysis in which a more intense probe pulse removes many electrons from the molecular cation, initiating fragmentation. This is in contrast to the previous scheme in which a single electron was removed in the probe focus.

For CS_2 , Figure 6a depicts the net spectrum of detector arrival times for doubly charged parent and fragment ions. It was obtained by subtracting “pump pulse only” and “probe pulse only” spectra from that produced by the pump and probe pulses

together. Consequently, the net spectrum reflects only those ions produced via single ionization in the pump focus and subsequent multiple ionization in the probe focus. Numerous fragments (C^+ , C^{2+} , S^+ , S^{2+} , S^{3+} , CS^+) were observed. Coulomb explosion of the highly charged parent ions imparts large kinetic energies (on the order of tens of eV) to the fragments. As a result, fragment peaks in Figure 6a are considerably broader than that corresponding to unexploded CS_2^{2+} .

The net monatomic fragment signal (indicated by the shaded region in Figure 6a) as a function of ion acceleration voltage is shown in Figure 6b. For comparison, the voltage dependence of $^{76}CS_2^{2+}$ (recorded concurrently) is also shown. Note that Figure 6b is the Coulomb explosion analogue of Figure 5. Both the net fragment and $^{76}CS_2^{2+}$ signals maximize at the same voltage (Figure 6b) and yield the correct mass for the $^{76}CS_2$ parent molecule. The net fragment data contain more scatter than their unexploded counterparts due to the spectral subtraction procedure used to isolate the net fragment signal.

Finally, the magnitude of the net fragment peak was ~ 6 times that of the maximum $^{76}CS_2^{2+}$ signal. This was due in part to the ion signal amplification (i.e., the production of multiple fragments per molecule) inherent to Coulomb explosion detection. For larger polyatomic molecules, the amplification should increase substantially.

DISCUSSION AND CONCLUSIONS

Using our optical approach, it should be possible to construct a relatively simple miniature mass spectrometer. Miniaturization greatly relaxes requirements for power sources, vacuum, and detection electronics. In our demonstration, the potential difference between the pump and probe foci was only ~ 5 V. For a pair of closely spaced (~ 1 mm) electrodes, a household battery can provide an equivalent acceleration field.

While a high-vacuum environment was required in our long spectrometer to prevent ion collisions with background gas, only rough vacuum is required for the submillimeter flight distances of a miniature device. Therefore, an actual device could be made highly portable if a rudimentary pump is used to provide evacuation. A further requirement for such a device is that the

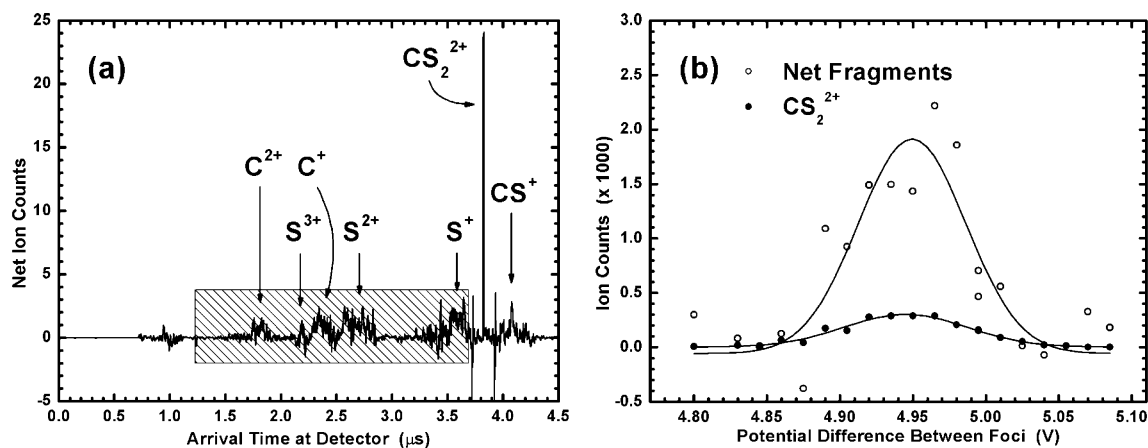


Figure 6. (a) Net spectrum of arrival times at the detector for the dication and charged fragments of CS_2 . The spectrum was obtained by subtracting the individual arrival time spectra for the pump and probe pulses used alone from that produced using the two pulses concurrently. The integration window for fragment signal measurement is also shown (hatched region). (b) Integrated CS_2 fragment (hollow circles) and CS_2^{2+} (filled circles) signals as a function of potential difference between foci are shown. The peak voltages of the two signals effectively coincide, thereby demonstrating the validity of Coulomb explosion detection. The net fragment counts are many times greater than the unenhanced CS_2^{2+} signal, due in part to the amplification inherent to Coulomb explosion detection.

initial velocity of molecules in the pump focus toward the detector be minimal. This constraint was satisfied in our demonstration using a molecular beam but could be met in a miniature device by placing the pump focus on the axis of an effusive molecular jet or by combining the miniature spectrometer with a microlaser desorption source.

Pulse intensity is the critical parameter in strong-field ionization. To implement our optical approach, respective pump and probe intensities of $\sim 1 \times 10^{14}$ and 2×10^{14} W/cm² are required.⁸ Commercially available 10-fs oscillators operate at a peak intracavity power of $\sim 5 \times 10^6$ W and often incorporate intracavity foci. Therefore, it should be possible to attain an intracavity intensity of $\sim 5 \times 10^{14}$ W/cm² and perform mass spectrometry at 10^8 Hz using relatively simple lasers. The high repetition rates of such lasers would compensate for the loss of the multiplex advantage intrinsic to electronically timed time-of-flight mass spectrometers.

The use of two synchronized lasers would eliminate the need for a long optical delay line and make the optical configuration quite simple and compact (Figure 2). The pump and probe pulses could be delivered via optical fibers and focused by microlenses mounted on the fiber tips. With diffraction-limited $f/1$ focusing, 1- μJ pulses from fiber-based laser systems would be more than adequate to implement Coulomb explosion detection. Currently, such lasers are commercially available as compact turnkey systems with footprints of just ~ 200 cm². Thus, there are numerous options for the lasers required to perform optically timed mass spectrometry.

During the Coulomb explosion process, numerous ionic fragments are produced per molecule. Since highly charged fragments can be produced,⁶ the number of free electrons can be even larger. For large polyatomic molecules, these inherent

amplifications of detectable particles could be large⁶ and make concurrent detection of electrons and fragments feasible using a pair of simple electrodes and a current amplifier. Consequently, Coulomb explosion detection represents one of the most important potential applications of femtosecond mass spectrometry.

In addition to enabling the performance of compact mass spectrometry, our optical approach provides the basis for a submillimeter-scale mass selector with potential applications in ion physics. This is demonstrated in Figure 4, where an appropriate choice of experimental parameters enhanced the central triplet's $^{76}\text{CS}_2^{2+}$ signal relative to the $^{77}\text{CS}_2^{2+}$ and $^{78}\text{CS}_2^{2+}$ peaks. Experiments on ion ensembles devoid of neutrals are typically performed using a tandem mass spectrometer that incorporates separate stages for ion production, selection, and postinteraction analysis.¹¹ By using our two foci for ion production and selection, we have demonstrated all three of these functions within a single time-of-flight spectrometer and reduced the commonly used tandem spectrometric configuration to a more compact, nested one.

Our nested spectrometric configuration has many scientific applications. The most important may be in lifetime measurements of transient ion species. In conventional measurements, ion lifetimes are determined from the structure of their mass peaks and the resolution is on the order of the flight time. Since our approach enables the performance of mass analysis over submillimeter distances with nanosecond flight times, the accuracy of transient lifetime measurements could be enhanced using our configuration.

Received for review June 6, 2003. Accepted October 22, 2003.

AC034621X

(11) de Hoffmann, E. *J Mass Spectrom.* **1996**, *31*, 129–137.